Journal of Nano- and Electronic Physics
Vol. **15** No 2, 02001(9pp) (2023)

Журнал нано- та електронної фізики
Том **15** № 2, 02001(9cc) (2023)

Organic Field Effect Transistor Based on Adaptive Neuro-Fuzzy Inference System

Imad Benacer[1,*], Fateh Moulahcene[1], Fateh Bouguerra[2], Ammar Merazga[1]

[1] *Institute of Science and Applied Technology (SAT Institute), University Of Oum El Bouaghi, Algeria*
[2] *Department of Electronics, University of Batan 2, Batna, Algeria*

(Received 05 December 2022; revised manuscript received 20 April 2023; published online 27 April 2023)

Organic Field-Effect Transistors (OFETs) attract much interest recently and their proficiency and hence applications are being enhanced increasingly. The device simulation was performed using finite element two dimensional drift-diffusion simulations, the results obtained are compared with experiments data and a good match has been observed between them. This paper introduces a method for modeling the OFET based on Adaptive Network Fuzzy Inference System (ANFIS) approach, the required data for training of ANFIS has been obtained using Atlas 2D device simulator. Finally, we imported the ANFIS model in a circuit simulator like PSPICE, simulation results of the developed ANFIS subcircuit have indicated that the proposed fuzzy logic based approach model is suitable to be incorporated in PSPICE-like tools for OFET circuits simulation.

Keywords: Organic Field Effect Transistors (OFET), Poole-Frenkel mechanism, Adaptive neuro-fuzzy inference system (ANFIS), PSPICE.

DOI: 10.21272/jnep.15(2).02001 PACS number: 85.30.Tv

1. INTRODUCTION

Recently there has been remarkable interest on organic electronics due to their advantages if we compare it with inorganic electronics. First of all, it can be fabricated at low temperature and at considerably low cost [1]. Secondly it is thin, lightweight, foldable, bendable, strong optical absorption, unbreakable, mechanical flexibility, consumes much less energy and efficient emission [2]. Thirdly, it has low cost due to cheaper material and lower cost deposition process techniques. Finally it can be used for large area applications [3]. Organic electronics have shown potential for many applications such as low cost flexible displays, radio frequency identification tags (RFIDs), sensors, Mobile phones, leading research interest worldwide [4].

The performance of Organic Field Effect transistor (OFET) has continuously improved since then, and some OFETs now compete with amorphous silicon FETs, which are now preferred to conventional crystalline silicon FETs in applications where large areas are needed [5]. OFET performances are mainly limited by poor charge mobility in organic materials, and nonlinear charge injection efficiency from the electrodes to the transistor channel (high contact resistance) [6-7]. Majority of OFETs, that have been reported in literature are p-type devices such as pentacene due to high mobility [8]. Improvements the performance of OFETs not depends only on mobility but there are other ways such as scaling of channel length and variation in active layer thickness [9-10]. OFETs have been fabricated with various device geometries. The most commonly used device geometry is bottom gate with top or bottom drain and source electrodes (BGTC-BGBC), because the deposition of organic semiconductor on the insulator is much easier than the reverse due to fragile nature of organic semiconductor materials, this is the reason that gives preference to the bottom gate structure to built in majority for current OFETs. On the other hand, the performance degrades in bottom contact (BC) due to high contact resistance which enables lower currents for the same applied voltages in comparison to the TC structure [11-12].

Device modeling for circuit simulation is usually done through compact models, which tray to model the physical phenomena inside the device that uses either physically based functions or empirical functions. When fast modeling is required and we are not concerned about the physics inside the device, the easy modeling approach in dealing with nonlinear systems is to use non-linear methods such as Adaptive Network Fuzzy Inference System (ANFIS). With the accuracy of the ANFIS model in the simulation of the OFET, we can use the ANFIS as a neuro-fuzzy behavioral model in a PSPICE simulator after identifying the ANFIS equations with appropriate syntax. In this paper, top contact device configuration of OFET was studied using Silvaco ATLAS two-dimensional (2-D) numerical device simulator [13]. We present a method for modeling the OFET based on computational intelligence technique (ANFIS). The ANFIS could be used to provide a link from measurements or device simulations to circuit simulation. Here, we propose a technique to include OFET devices in PSPICE making use of adaptive neuro fuzzy training systems.

The data set used for the training of our fuzzy system is obtained by the numerical simulator ATLAS, which can be used as the target data set for optimizing the ANFIS architecture. Our intention is to provide a framework to facilitate the simulation on OFET based circuits.

2. DEVICE SIMULATION TECHNIQUES

2.1 Finit Element Based Atlas Simulation

Comparative studies were conducted through physically based 2D device simulation. This simulator is able

* benacerimad@gmail.com, benacer.imad@univ-oeb.dz

to predict electrical characteristics of the device given its physical structure and bias conditions by solving simultaneously the Poisson's equation for electrical potential and the continuity equation for hole and electron concentrations including drift and diffusion terms [13]. The simulation was done with a one-carrier model of the hole, Poisson's and carrier continuity equations given for holes by (Eq. 2.1) and (Eq. 2.2) below:

$$\varepsilon \nabla^2 \psi = -p\ q \tag{2.1}$$

$$\frac{\partial p}{\partial t} = \frac{1}{q}\nabla \cdot j_p + G_p - R_p \tag{2.2}$$

where, ε is dielectric constant, ψ is potential profile, p is hole density, q is the unit charge, G_p is carrier generation rate, R_p is the carrier recombination rate, and J_p is the hole current density which is given considering its drift and diffusion components as:

$$j_p = pq\mu_p F + qD_p \nabla_p \tag{2.3}$$

where μ_p is the mobility of holes, F is the electric field, and D_p is the hole diffusion coefficient. This simulator was primarily developed for silicon devices or compound semiconductor devices, but it can be applied to organic devices such as OLEDs and OTFTs.

Fig. 1 shows the structure of the simulated OFET based on top contact configuration. These devices have channel length L of 10 μm and a channel width W of 100 μm, with 30 nm thick film of pentacene and 5.7 nm thick dielectric gate as indicated in [14]. The charge transport model used for pentacene was Poole–Frenkel model which is expressed as

$$\mu = \mu_0 \exp\left(-\frac{\Delta E_a - \beta\sqrt{E}}{K_B T}\right) \tag{2.4}$$

The zero field activation energy (ΔEa) of pentacene equal to 0.018 eV. The Poole-Frenkel factor, β was 3.58×10^{-5} eV(cm/V)$^{0.5}$, K_B is the Boltzmann constant and T is the temperature, a positive interface charge of approximately q × 1 × 10^{12} C·cm^{-2} (q is the unit charge) at insulator/pentacene interface was used for the simulation [12, 15].

Table 1 – Simulation parameters [8-9]

Material (layer)	Parameter	Value
Pentacene	Band gap	2.2 eV
	Density of conduction band	2×10^{21} cm^{-3}
	Density of valence band	2×10^{21} cm^{-3}
	Permittivity	4.0
	Acceptor doping concentration	4×10^{17} cm^{-3}
	Affinity	2.8 eV
AlO_x (Gate insulator)	Dielectric constant	4.5
	Thickness	5.7 nm
Au (source/drain contact)	Work function	5.0 eV

Constant density of states, 2×10^{21} cm^{-3}, at room temperature has been used in the conduction and valence bands of pentacene. In the literature, values of the effective density of the states, N_c and N_v, ranging from 10^{19} to 6×10^{21} cm^{-3} have been reported for pentacene [16]. The work function of the source, drain and gate electrode is assumed to be 5.0 eV.

Table 1 summarizes the parameters values (dimensions, material and model parameters) used for the modeling of the transistor based on numerical simulation.

2.2 Results and Discussion

OFETs can operate in the electron or hole carrier accumulation modes depending on the polarity of the gate voltage. Pentacene acts as a p-type semiconductor where majority carriers are holes. When a negative gate voltage is applied, an electric field is formed across the dielectric, causing an accumulation region of holes at the dielectric-pentacene interface. Applying a voltage to source-drain terminals allows a current to flow across this accumulation layer between the contacts.
Figs. 1a and 1b show the contour images of the current flow path distribution in the high-current condition of the saturation regime ($V_{gs} = V_{ds} = -3$ V), it can be easily understood from current flow lines, that charge injection is taking place from side/corner of the contacts and charge transport occurs in the first few layers adjacent to the dielectric.

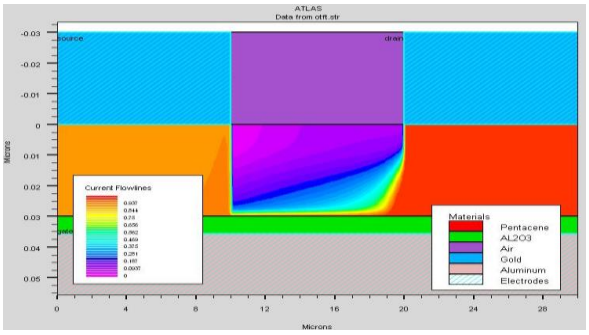

a

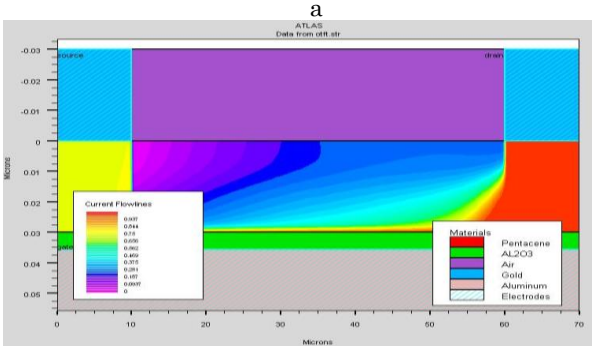

b

Fig. 1 – Schematic diagram for the current flow path distribution in pentacene film ($V_{gs} = V_{ds} = -3$ V) with channel lengths of 10 μm (a), 50 μm (b)

Figs. 2a and 2b present comparisons between experimental data [14] and the drain current simulated by Silvaco of OFET with channel lengths of 10 μm, 20 μm, and 50 μm respectively. It can be observed that we have a good agreement between experimental and sim-

ulated values. Fig. 3 compares experimental data [14] and numerical results (Silvaco) of the current–voltage characteristics (I_D-V_{GS}) for an OFET with channel length ranging from 10 to 50 μm in the low-current condition of the linear regime, as it can be seen, the best agreement between them is obtained in full range. The saturation current value of the channel length of 10 μm is four times higher than that of the 50 μm

As shown in Fig. 2 and Fig. 3 it is clear that drain current increases with decreasing of channel length due to reduction of channel resistance.

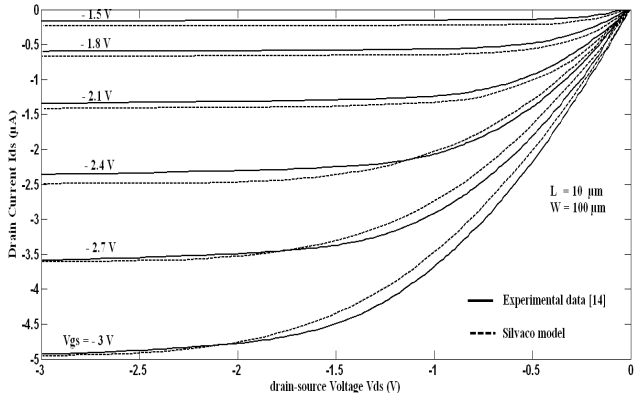

a

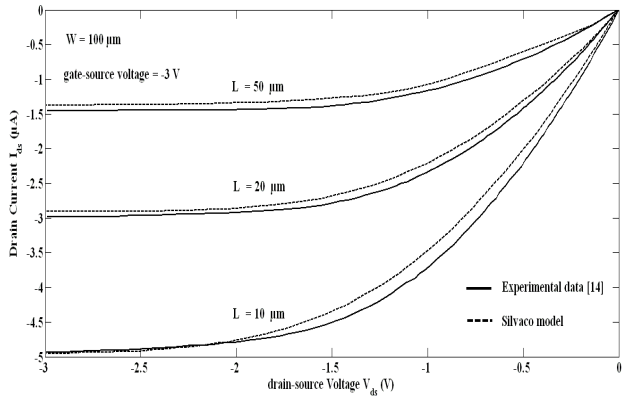

b

Fig. 2 – Comparison of experimental and simulated (dashed line) output characteristics of OFET with channel lengths of 10 μm (a), 10, 20 and 50 μm (b)

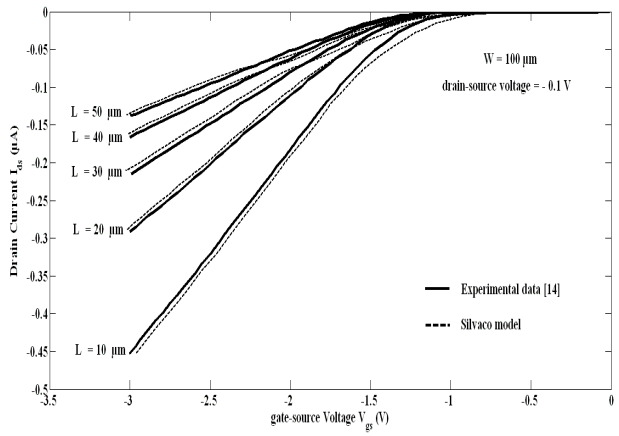

Fig. 3 – Comparison of experimental and simulated (dashed line) transfer characteristics of OFET at different channel lengths

2.3 ANFIS Methodology

ANFIS is an adaptive network which combines the application of neural network and fuzzy logic to achieve all of the advantages of both systems [17-18]. This method based on the input-output data of the system under consideration.

The main objective of the ANFIS is to determine the optimum values of the equivalent fuzzy inference system parameters by applying a learning algorithm using input-output data, thus get a good matching between the predicted and measured responses. The hybrid learning algorithm for ANFIS has been used in this study, which is a combination of back-propagation gradient descent and the least-squares method to identify and optimize the Sugeno system's signals [19-20]. ANFIS architecture of a first order Sugeno fuzzy model is shown in Fig. 4. It should be noted that the circle indicates a fixed node, whereas the square indicates an adaptive node.

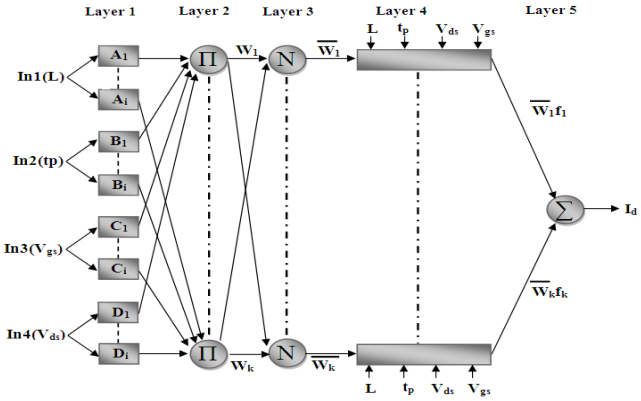

Fig. 4 – Structure of ANFIS proposed for the estimation of the drain current

In this paper, we have built the ANFIS model to relate input parameters (L, t_p, V_{ds} and V_{gs}) to output parameter I_d, where L is the channel length, t_p is the pentacene film thickness, V_{ds} is the drain-source voltage, V_{gs} is the gate-source voltage, and I_d is the drain current in OFET. The related illustration is shown in Fig. 5.

The generic expression of such fuzzy IF-THEN rules, in which the outputs are linear combinations of their inputs, is given by:

Rule k: IF L is A_i and t_p is B_i and V_{gs} is C_i and V_{ds} is D_i

THEN

$$f_k = p_k L + q_k t_p + h_k V_{gs} + g_k V_{ds} + r_k \qquad (2.5)$$

$i = 1, 2,\ldots n$, $k = 1, 2,\ldots m$

where A_i, B_i, C_i and D_i are linguistic labels for inputs, f_k is the output within the fuzzy region specified by the fuzzy rule, $\{p_k, q_k, h_k, g_k, r_k\}$ are linear output parameters that are determined during the training process, m is the total number of Takagi-Sugeno-Kang fuzzy IF-THEN rules, and n is the number of fuzzy sets attached to each input.

The corresponding ANFIS architecture is composed of interconnected nodes organized in five functional layers as follows:

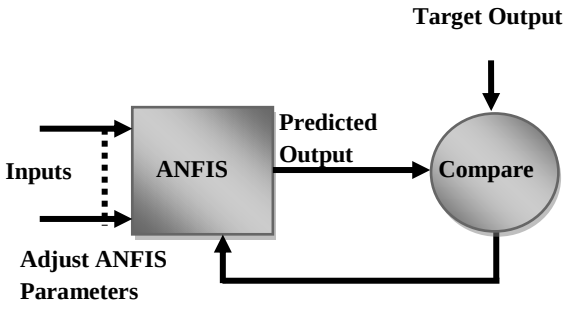

Fig. 5 – Overview of the proposed model block diagram

Layer 1: Each node in this layer is an adaptive node and that generates membership grades of a linguistic label.

The number of the membership functions for the input parameters is fixed to 3 for each input, which gives a number of fuzzy IF-THEN rules for the fuzzy inference system equals to 81 ($3 \times 3 \times 3 \times 3$). The output in layer 1 defined by:

$$\begin{cases} O_{1,i} = \mu_{Ai}(L), & i = 1,2,3 \\ O_{1,i} = \mu_{Bi-3}(t_p), & i = 4,5,6 \\ O_{1,i} = \mu_{Ci-6}(V_{gs}), & i = 7,8,9 \\ O_{1,i} = \mu_{Di-9}(V_{ds}), & i = 10,11,12 \end{cases}$$

where i is the membership grade of a fuzzy set (A_i, B_i, C_i, D_i) and $O_{1,i}$ is the output of the node i in layer l. The membership function that has been used in this study is the Gaussian function given by:

$$o_1 = \mu_{Ai}(x) = \exp\left(\frac{-0.5(x-c)^2}{\sigma^2}\right) \qquad (2.6)$$

where c and σ are the premise parameter set used to adjust the shape of the membership function.

Layer 2: Each node in this layer is a fixed node labeled Π and calculates the firing strength of a rule via multiplication. The outputs are given by:

$$O_{2,k} = \mu_{Ai}(L).\mu_{Bi-3}.(t_p).\mu_{Ci-6}(V_{gs}).\mu_{Di-9}(V_{ds}) = W_k \quad (2.7)$$

$K = 1, 2, \ldots m$

Layer 3: Every node in this layer is also fixed node labeled N and presents a normalization of the firing strength from the previous layer. The outputs of this layer are called normalized firing strengths and are given by

$$o_{3,k} = \overline{w_k} = \frac{w_k}{\sum_{l=1}^{m} w_l} \qquad (2.8)$$

$K = 1, 2, \ldots m$

Layer 4: In this layer, all nodes are adaptive. The relationship between the inputs and output of this layer can be defined as the following:

$$o_{4,k} = \overline{w_k} f_k = \overline{w_k}\left(p_k L + q_k t_p + h_k V_{gs} + g_k V_{ds} + r_k\right) \quad (2.9)$$

where $\overline{w_k}$ is a normalized firing strength from layer 3, and $\{p_k, q_k, h_k, g_k, r_k\}$ is the consequent parameter set of the node.

Layer 5: this layer contains only a single node that calculates the overall ANFIS output from the sum of the node inputs

$$o_{5,1} = \sum_{k=1}^{m} \overline{w_k} f_k = \frac{\sum_{k=1}^{m} w_k f_k}{\sum_{k=1}^{m} w_k} \qquad (2.10)$$

We present the basic theory of ANFIS model, both artificial neural network and fuzzy logic are used in ANFIS architecture.

2.4 Results and Discussion

The required data for training of ANFIS has been obtained using Atlas 2D device simulator (15000 samples). To check the generalization ability of the model, cross-validation method is used [21]. The data set of the device available is divided into two subsets: the training set and the validation set.

Cross-validation methods help find parameter estimates that can generalize to unseen data by periodically testing the current model on a validation set. The algorithm K-fold cross-validation splits the data into k equal size subsets randomly, a single subset is retained as the validation data for testing the model, and the remaining K^{-1} subsets are used as training data, the method is repeated K times (the folds). Every data point appears in a test set only once and appears in a training set twice, in this paper, we use 5-fold cross validation.

The minimum and maximum input data ranges used for building the ANFIS model is shown in Table 2.

Table 2 – Data ranges used for building the proposed ANFIS model

Rang	L(μm)	t_p(nm)	V_{ds}(V)	V_{gs}(V)
Min	10	20	0	0
Max	50	30	– 3	– 3

The performance of ANFIS model is assessed by evaluating the differences between the simulated and predicted values by the correlation coefficient (R) and root mean square error (RMSE)

$$RMSE = \frac{1}{N}\sum_{i=1}^{N}\left(\frac{X_{i,Num} - X_{i,\mathrm{Pred}}}{X_{i,Num}}\right)^2 \qquad (2.11)$$

where X_{Num} and X_{Pred} stand for numerical (Silvaco simulation) and predicted (ANFIS) values, respectively, and N is the number of data. The parameter optimization is done in such a way during training phase that the error between the target and the output of ANFIS is minimized to get a good matching between the predicted and measured responses. A sufficient agreement is satisfied between numerical and predicted results for the training phase, as shown in Fig. 6.

The final ANFIS architecture used in this paper is shown in Table 3.

Table 3 – Specifications of proposed ANFIS model

Item	Specification
Inputs/outputs	4/1
FIS Type	Sugeno
Train FIS method	hybrid
Input MF Type	Gaussian mf
Output Membership Function Type	Linear
No. of fuzzy rules	81
Epochs	200

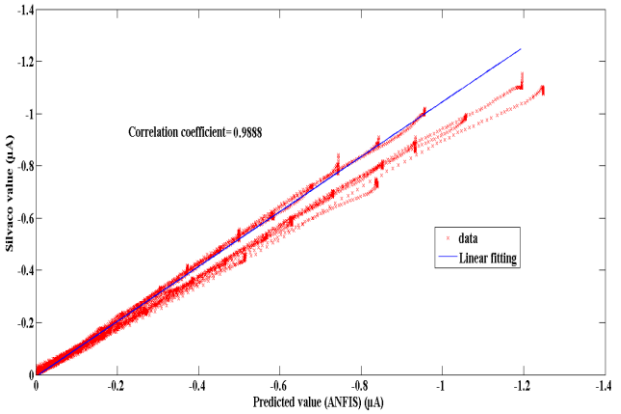

Fig. 6 – Comparison of the Silvaco and predicted ANFIS results for training data

As mentioned previously, the number of the membership functions for the input parameters is fixed to 3 for each input. ANFIS system is sensitive to number of membership function, giving additional number of membership function to the system did not always improve the result, as well as to simplicity of the ANFIS model to be incorporated in PSPICE-like tools (Section 3).

The examination of the obtained results indicates that the use of the Gaussian-Shaped membership function gives higher performances compared to the others membership functions. The best membership function configuration is illustrated in Fig. 7.

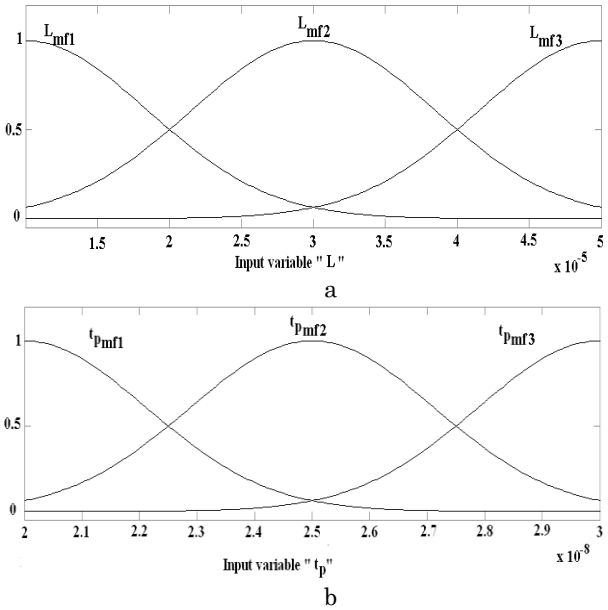

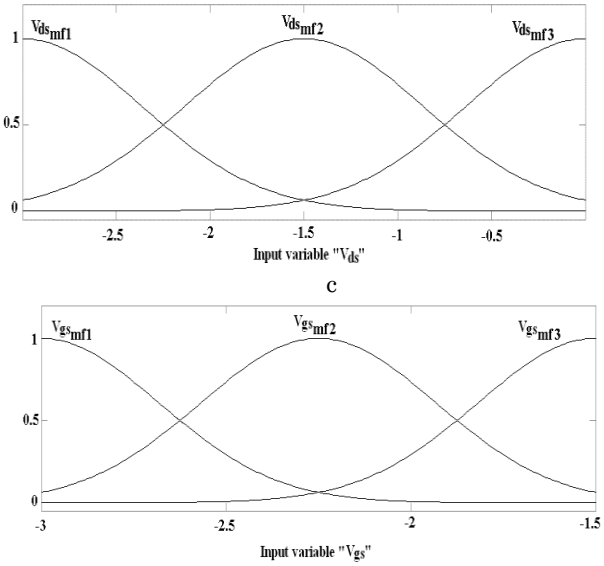

Fig. 7 – Gaussian membership functions of the channel length (a), pentacene film thickness (b), drain-source voltage (c), gate-source voltage parameters (d)

Fig. 8 depicts the response surface of the obtained ANFIS where the drain current is plotted as a function of both drain-source voltage (V_{ds}) and gate-source voltage (V_{gs}). As shown from the graph of Fig. 8 the drain current increases with V_{gs}.

The response surface of the obtained ANFIS of the variation in the drain current (output) with pentacene film thickness (t_p) (input 1) and channel length (L) (input 2) is shown in Fig. 9, it is clear that drain current increases with decreasing of channel length due to reduction of channel resistance.

Fig. 8 and Fig. 9, they present a similar behavior characterized by the device.

3. IMPLEMENTATION OF ANFIS TO PSPICE

After optimizing the proposed ANFIS structure, all parameters of input membership functions and output parameters obtained. In PSPICE implementation [22,23], we imported ANFIS model of OFET by using ABM (Analog Behavioral Modeling) of the PSPICE library components and the results (firing strength, rules, parameters of Gaussian input membership and linear output), the OFET model is implemented as a component in the PSPICE simulator library.

A simplified overview of our proposed approach block diagram is shown in Fig. 10a, which is describe the using of this model as the interface between device modeling and circuit simulators like PSPICE, Cadence, and SABER in order to have a simple and accurate organic circuits simulator. In Fig. 10b we show the PSPICE program which corresponds our ANFIS OFET model.

The development of electronic circuits is supported by powerful computer tools. An important tool for the development of such complex organic integrated circuits is simulation programs such as PSPICE (Personal Simulation Program with Integrated Circuit Emphasis) that allow for accurate prediction of the electrical behavior even while changing working conditions or varying internal parameters.

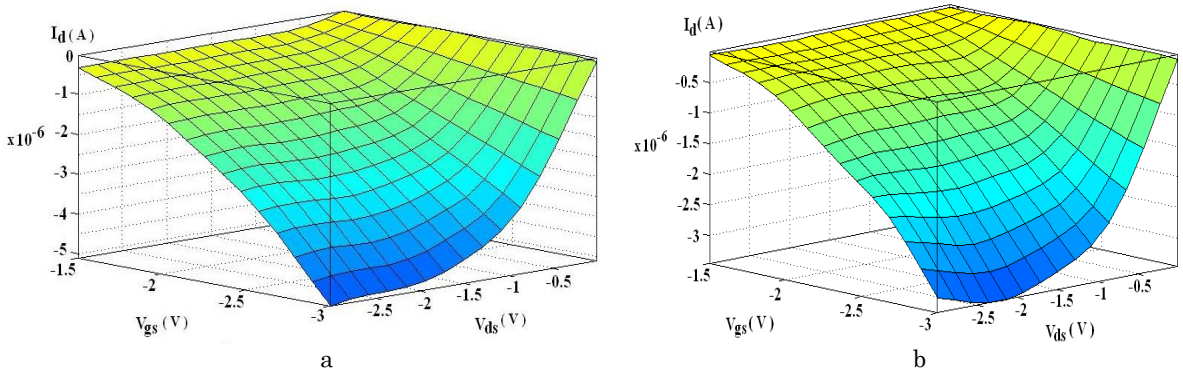

Fig. 8 – ANFIS controller rule surface for L = 50 μm and t_p = 30 nm (a), L = 10 μm and t_p = 20 nm (b)

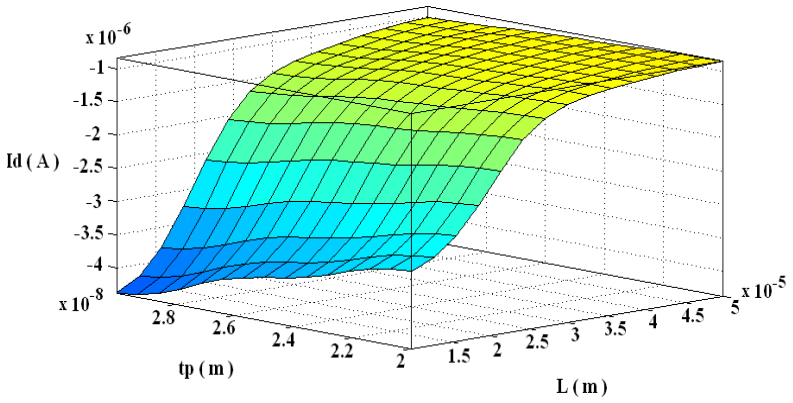

Fig. 9 – ANFIS controller rule surface for V_{gs} = -3 V and V_{ds} = -3V

Fig. 11a shows the ANFIS model circuit simulation in PSPICE. Fig. 11b shows the output characteristics for the ANFIS model with 10 μm channel length and 30 nm thickness of pentacene.

Fig. 12 compares Silvaco and predicted results of ANFIS PSPICE model to experiment results of the current-voltage characteristics (I_D-V_{DS} and I_D-V_{GS}) for an OFET with L = 10 μm and t_p = 30 nm, as it can be seen, the best agreement between them is obtained in full range.

As verification for our ANFIS model, a circuit simulation of a resistor load inverter (see Fig. 13a) with a 10 μm channel length transistor has been performed. The PSPICE input/output signals of our ANFIS inverter gate are shown in Fig. 13b. The transient simulation results presented verify the functionality of our model. So, we can use this model for simulating more complex OFET based circuits.

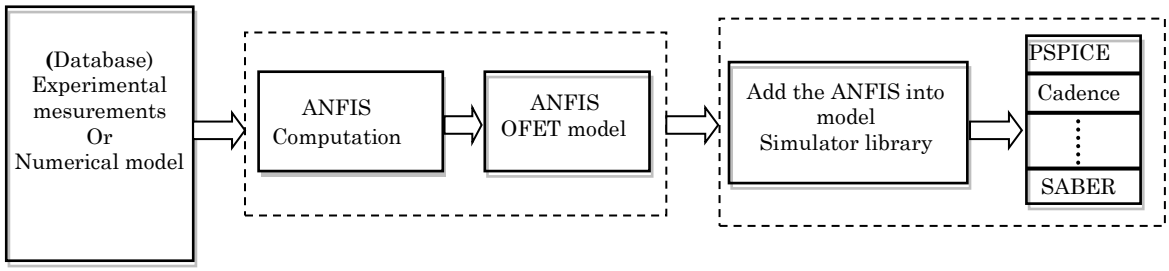

a

```
* source ANFIS
.EXTERNAL INPUT L
.EXTERNAL INPUT TP
.EXTERNAL INPUT VDS
.EXTERNAL INPUT VGS
.EXTERNAL OUTPUT Id
* Ci and σi are the premise parameter set used to adjust the shape of the membership function
*{pk,qk,hk,gk,rk} is the consequent parameter set of the node
* first layer
E_ABM1      N2528094 0 VALUE {exp(-0.5*(pwr(V(L)-C1,2))/pwr(σ1,2))}
E_ABM2      N2528094 0 VALUE {exp(-0.5*(pwr(V(L)-C2,2))/pwr(σ2,2))}
E_ABM3      N2528094 0 VALUE {exp(-0.5*(pwr(V(L)-C3,2))/pwr(σ3,2))}
E_ABM4      N2527850 0 VALUE {exp(-0.5*(pwr(V(TP)-C4,2))/pwr(σ4,2))}
E_ABM5      N2528542 0 VALUE {exp(-0.5*(pwr(V(TP)-C5,2))/pwr(σ5,2))}
E_ABM6      N2528002 0 VALUE {exp(-0.5*(pwr(V(TP)-C6,2))/pwr(σ6,2))}
E_ABM7      N2531486 0 VALUE {exp(-0.5*(pwr(V(VDS)-C7,2))/pwr(σ7,2))}
E_ABM8      N2527780 0 VALUE {exp(-0.5*(pwr(V(VDS)-C8,2))/pwr(σ8,2))}
E_ABM9      N2529274 0 VALUE {exp(-0.5*(pwr(V(VDS)-C9,2))/pwr(σ9,2))}
E_ABM10     N2528530 0 VALUE {exp(-0.5*(pwr(V(VGS)-C10,2))/pwr(σ10,2))}
E_ABM11     N2528506 0 VALUE {exp(-0.5*(pwr(V(VGS)-C11,2))/pwr(σ11,2))}
E_ABM12     N2527792 0 VALUE {exp(-0.5*(pwr(V(VGS)-C12,2))/pwr(σ12,2))}
* Second layer
E_ABM13      N2527898 0 VALUE { V(N2531486)*V(N2528530)*V(N2528226)*V(N2527850)}
E_ABM14      N2532768 0 VALUE { V(N2531486)*V(N2528530)*V(N2528226)*V(N2528542)}
E_ABM15      N2528230 0 VALUE { V(N2531486)*V(N2528530)*V(N2528226)*V(N2528002)}
*
*
*
E_ABM93      N2536552 0 VALUE { V(N2529274)*V(N2527792)*V(N2528094)*V(N2528002)}
* Third layer
E_ABM94      N2535008 0 VALUE { V(N2527898)* (p1*V(L)+q1*V(TP)+g1*V(VDS)+h1*V(VGS) +r1)}
E_ABM95      N2536780 0 VALUE { V(N2532768)* (p2*V(L)+q2*V(TP)+g2*V(VDS)+h2*V(VGS) +r2)}
E_ABM96      N2538472 0 VALUE { V(N2528230)*(p3*V(L)+q3*V(TP)+g3*V(VDS)+h3*V(VGS) +r3)}
*
*
*
E_ABM174      N2527994 0 VALUE { V(N2536552)*(p81*V(L)+q81*V(TP)+g81*V(VDS)+h81*V(VGS) +r81)}
* Fourth layer
E_ABM175      N2626318 0 VALUE {V(N2535384)+V(N2537228)+
+V(N2539176)+V(N2528346)+.....V(N2535268)+V(N2537448)+V(N2527994)}
* Fifth layer
E_ABM176      N2682453 0 VALUE {V(N2527898)+V(N2532768)+V(N2528230)
++V(N2539176)+V(N2528346)+.....V(N2535268)+V(N2537448)+V(N2527994)}
* Output layer
E_ABM177      N2530464 0 VALUE {(V(N2657647)/V(N2650810))}
```

b

Fig. 10 – Our proposed approach block diagram (a), PSPICE program of ANFIS OFET model (b)

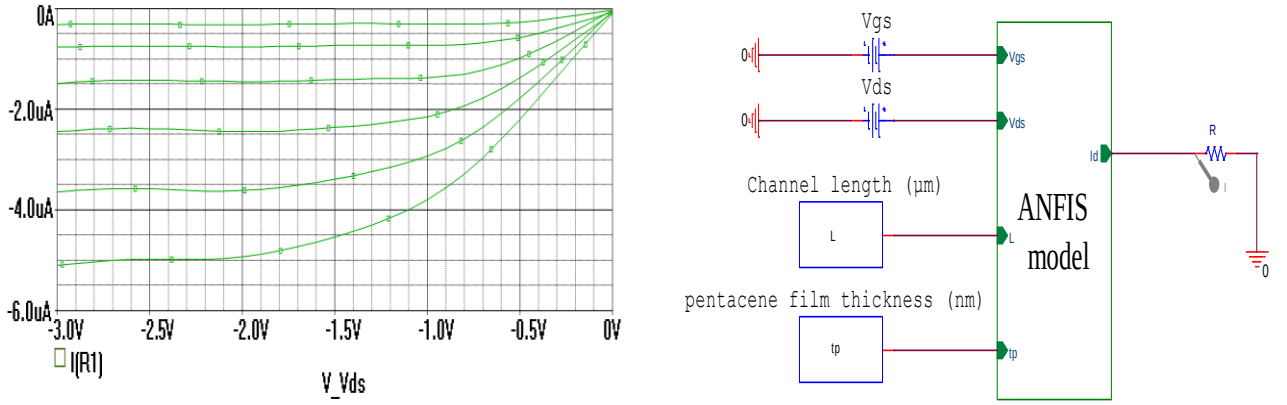

a b

Fig. 11 – ANFIS model circuit simulation in PSPICE (a), the PSPICE output characteristics of our ANFIS model (L = 10 μm and t_p = 30 nm) (b)

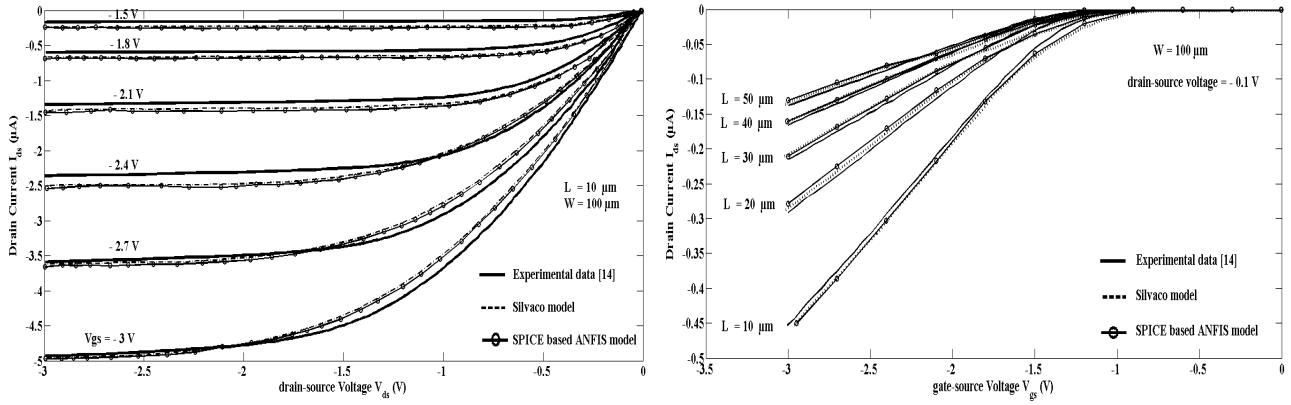

a b

Fig. 12 – Comparison of experimental and simulated (a) Output characteristics of OFET with channel lengths of 10 µm (a), transfer characteristics at different channel lengths (b)

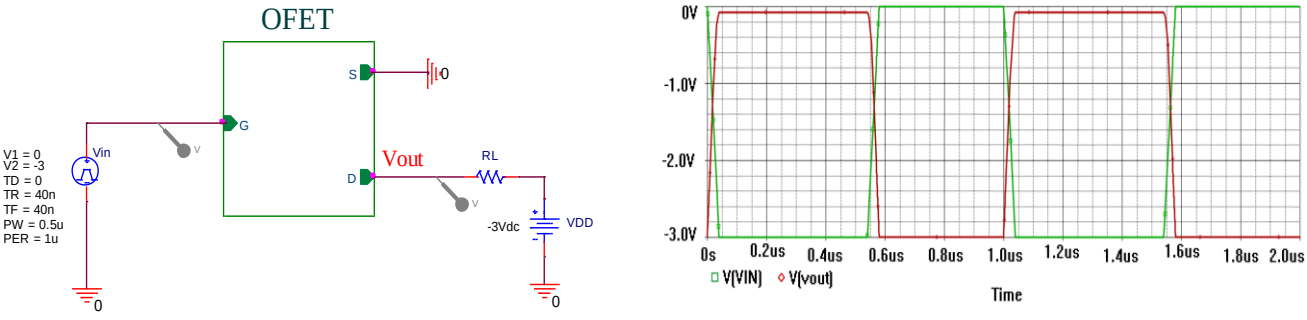

a b

Fig. 13 – The PSPICE circuit of transistor load inverter (a), the PSPICE input and output signals of our ANFIS inverter (b)

4. CONCLUSION

In this paper, the application of an ANFIS for modeling and simulation of organic field effect transistor has been demonstrated. A numerical model of the current-voltage characteristics was built based on the 2D-ATLAS simulator, with this numerical model the required training database has been created, where a hybrid learning algorithm has been used to adjust various premise and consequent parameters.

The simulation results by PSPICE have shown that the proposed fuzzy logic based approach model is suitable to be incorporated in PSPICE-like tools for OFET circuits simulation. ANFIS is a powerful fuzzy logic neural network, which provides an efficient tool for modeling and simulation of the organic transistor circuits.

As perspective, the proposed framework can be extended to include other device parameters such as the dielectric gate thickness, contact resistance, and channel resistance, which offer the possibility of modeling the device behavior with more precision.

REFERENCES

1. B. Kumar, B.K. Kaushik, Y.S. Negi, Poornima Mittal, *IEEE Recent Advances in Intelligent Computational Systems (RAICS)*, 706 (2011).
2. B. Kumar, B.K. Kaushik, Y.S. Negi, Poornima Mittal, *IEEE Com. Systems and Network Technologies (CSNT)*, 436 (2011).
3. K. Brijesh, B.K. Kaushik, Y.S. Negi, P. Mittal, *Proc. IEEE Int. Conf. on Electrical and Computer Technology (ICETECT)*, 702 (2011).
4. P. Mach, S.J. Rodriguez, R. Nortrup, P. Wiltzius, J.A. Rogers, *Appl. Phys. Lett.* **78**, 3592 (2001).
5. C.D. Dimitrakopoulos, P.R.L. Malenfant, *Adv. Mater.* **14** No 2, 99 (2002).
6. I.G. Hill, *Appl. Phys. Lett.* **87**, 163505 (2005).
7. O. Simonetti, L. Giraudet, T. Maurel, J.-L. Nicolas, A. Belkhi, *Organic Electron.* **11** No 8, 1381 (2010).
8. J.B. Koo, J.W. Lim, S.H. Kim, S.J. Yun, C.H. Ku, S.C. Lim, J.H. Lee, *Thin Solid Films* **515** No 5, 3132 (2007).
9. P. Mittal, B. Kumar, B.K. Kaushik, Y.S. Negi, B.K. Kaushik, R.K. Singh, *Organic Electron.* **43** No 12, 985 (2012).
10. D. Gupta, Y. Hong, *Organic Electron.* **11** No 1, 127 (2010).
11. Y. Ishikawa, Y. Wada, T. Toyabe, *J. Appl. Phys.* **107** No 5, 053709 (2010).
12. D. Gupta, M. Katiyar, D. Gupta, *Organic Electron.* **10** No 5, 775 (2009).
13. *ATLAS User's Manual: Device simulation software.* Silvaco International, Santa Clara, CA (January 18, 2012).
14. H. Klauk, U. Zschieschang, M. Halik, *J. Appl. Phys.* **102**, 074514 (2007).
15. C. Shim, F. Maruoka, R. Hattori, *IEEE Trans. Elect. Dev.* **57** No 1, 195 (2010).
16. R. Schroeder, L.A. Majewski, M. Grell, *Appl. Phys. Lett.* **83**, 3201 (2003).
17. J. Jang, *IEEE Trans. Systems, Man Cybernytics* **23** No 3,

665 (1993).
18. J.-S.R. Jang, *Neuro-Fuzzy and Soft Computing, Prentice-Hall* (New Jersey: 1997).
19. R. Babuska, *Fuzzy Modeling for Control, Norwell, MA: Kluwer* (Academic Publishers: 1998).
20. J.-S.R. Jang, C.-T. Sun, *Proc. IEEE* **83** No 3, 378 (1995).
21. A.A. Najah, A. El-Shafie, O.A. Karim, O. Jaafar, *Neural Comput. Appl.* **21** No 5, 833 (2012).
22. M. Hayati, M. Seifi, A. Rezaei, *ETRI Journal* **32** No 4, 530 (2010).
23. F. Djeffal, M. Chahdi, A. Benhaya, M.L. Hafiane, *Solid-State Electron.* **51** No 1, 48 (2007).

Органічний польовий транзистор на основі адаптивної системи з нейро-нечітким виводом

Imad Benacer[1], Fateh Moulahcene[1], Fateh Bouguerra[2], Ammar Merazga[1]

[1] *Department of Telecommunication and Networking, University of Oum El-Bouaghi, Aïn M'lila, Algeria*
[2] *Department of Electronics, University of Batan 2, Batna, Algeria*

Органічні польові транзистори (OFET) останнім часом викликають великий науковий інтерес, а їх функціональність зростає. Моделювання пристрою було виконано з використанням кінцевого елементу двовимірного моделювання дифузійного дрейфу, отримані результати порівнюються з експериментальними даними, і між ними спостерігається хороша відповідність. У даній роботі представлено метод моделювання транзисторів OFET на основі підходу адаптивної мережевої системи нечіткого висновку (ANFIS). Вихідні дані для навчання ANFIS були отримані за допомогою симулятора пристроїв Atlas 2D. Автори імпортували модель ANFIS у симулятор схеми PSPICE, результати моделювання розробленої підсхеми ANFIS показали, що запропонована модель підходу на основі нечіткої логіки підходить для включення в PSPICE-подібні інструменти для моделювання схем транзисторів OFET.

Ключові слова: Органічні польові транзистори (OFET), Механізм Пула-Френкеля, Адаптивна нейро-нечітка система логічного виводу (ANFIS), PSPICE.